Effective core potential methods for the lanthanides

Thomas R. Cundari, and Walter J. Stevens

Citation: The Journal of Chemical Physics **98**, 5555 (1993);
View online: https://doi.org/10.1063/1.464902
View Table of Contents: http://aip.scitation.org/toc/jcp/98/7
Published by the American Institute of Physics

Articles you may be interested in

Compact effective potentials and efficient shared-exponent basis sets for the first- and second-row atoms
The Journal of Chemical Physics **81**, 6026 (1998); 10.1063/1.447604

Ab initio effective core potentials for molecular calculations. Potentials for the transition metal atoms Sc to Hg
The Journal of Chemical Physics **82**, 270 (1998); 10.1063/1.448799

Ab initio effective core potentials for molecular calculations. Potentials for K to Au including the outermost core orbitals
The Journal of Chemical Physics **82**, 299 (1998); 10.1063/1.448975

Density-functional thermochemistry. III. The role of exact exchange
The Journal of Chemical Physics **98**, 5648 (1998); 10.1063/1.464913

Ab initio effective core potentials for molecular calculations. Potentials for main group elements Na to Bi
The Journal of Chemical Physics **82**, 284 (1998); 10.1063/1.448800

Effective core potential studies of lanthanide complexes
The Journal of Chemical Physics **103**, 7058 (1998); 10.1063/1.470333

Effective core potential methods for the lanthanides

Thomas R. Cundari and Walter J. Stevens
Contribution from the Center for Advanced Research in Biotechnology, National Institutes of Standards and Technology, Rockville, Maryland 20850 and Department of Chemistry, Memphis State University, Memphis, Tennessee 38152

(Received 13 October 1992; accepted 14 December 1992)

In this paper a complete set of effective core potentials (ECPs) and valence basis sets for the lanthanides (Ce to Lu) are derived. These ECPs are consistent not only within the lanthanide series, but also with the third-row transition metals which bracket them. A 46-electron core was chosen to provide the best compromise between computational savings and chemical accuracy. Thus, the 5*s* and 5*p* are included as "outer" core while all lower energy atomic orbitals (AOs) are replaced with the ECP. Generator states were chosen from the most chemically relevant +3 and +2 oxidation states. The results of atomic calculations indicate that the greatest error vs highly accurate numerical potential/large, even-tempered basis set calculations results from replacement of the large, even-tempered basis sets with more compact representations. However, the agreement among atomic calculations remains excellent with both basis set sizes, for a variety of spin and oxidation states, with a significant savings in time for the optimized valence basis set. It is expected that the compact representation of the ECPs and valence basis sets will eventually encourage their use by computational chemists to further explore the bonding and reactivity of lanthanide complexes.

I. INTRODUCTION

Lanthanide chemistry, long neglected, has undergone tremendous growth in the recent past. The search for interesting chemistry of lanthanide compounds, complexes, and organometallics has been rewarded with highly reactive olefin polymerization catalysts,[1] the "first well-characterized example of the reaction of methane with a homogeneous organometallic complex,"[2] high temperature superconductors,[3] and novel biomedical reagents either for probing metabolic pathways[4] or as contrast reagents in magnetic resonance imaging.[5] It is safe to say, that despite the growing body of interesting lanthanide chemistry, that theory has lagged behind experiment, due in large part to well-known computational problems,[6,7] e.g., large numbers of orbitals and electrons, and the importance of relativistic and electron correlation effects.

Several computational approaches have been pursued for the lanthanides, including the extended Hückel studies of Hoffmann *et al.*,[8] semiempirical applications,[9] and *ab initio* treatments of workers such as Pyykko.[10] The use of effective core potentials (ECP) to replace core electrons, which do not partake in normal chemical reactions, has been quite successful for the treatment of the transition metals.[11] The ECPs can be derived to include relativistic effects, since their derivation can commence from Dirac–Hartree–Fock calculations. Indirectly, the correlation problem is also addressed since the computational resources saved by switching from an all-electron to ECP scheme can be dedicated to correlation. From the chemistry point of view, ECPs afford great leeway in the choice of interesting problems. For example, calculations on Sc-, Y-, La-, and the lanthanide (Ln) analogs of a catalyst can be studied with relatively similar computational effort, providing greater appreciation for trends as a function of the central metal in a complex. ECP schemes for the lanthanides have appeared in the literature.[12,13] Dolg *et al.* have derived Ln ECPs with various core sizes, including one in which 4*f* are treated as core electrons.[12] Ross *et al.* have derived potentials with a 54-electron (i.e., Xe) core.[13]

In the present contribution, we describe an extension of the scheme of Stevens *et al.*[14] for the derivation of effective core potentials and valence basis sets, providing a consistent set for the entire Periodic Table up to radon. The pertinent feature of this approach is the use of compact representations for the ECP and valence basis sets. Throughout, we use the transition metals, and known lanthanide chemistry, as a template in guiding various computational decisions. Note that we use the term lanthanide (Ln) to describe the elements from cerium ($Z=58$) to lutetium ($Z=71$). Lanthanum was treated previously with the transition metals.[14] The term rare earth is avoided since it typically includes the Sc-triad metals.

II. RESULTS AND DISCUSSION

A. Derivation of effective core potentials and valence basis sets for the lanthanides

The derivation of the ECPs and valence basis sets for the lanthanides follows closely the scheme of Stevens *et al.*[14] in their implementation for the transition metals. An overview of the derivation process is given below, with particular emphasis on those areas in which alterations to the previous recipe were deemed necessary given the different chemistry of the lanthanides.

 0021-9606/93/075555-11$06.00 © 1993 American Institute of Physics

1. Relativistic Dirac–Fock calculations

The first step in the derivation is a numerical Dirac–Hartree–Fock (DHF) calculation of an appropriate generator state for the fourteen lanthanides (Ce to Lu). The numerical DHF program due to Desclaux[15] was used for this purpose. Note that the one-electron Hamiltonian is fully relativistic, including the Darwin, mass-velocity and spin–orbit terms.

The most important decision at this stage is which state (oxidation or spin) of the atom to use in the ECP derivation. Test calculations, and previous experience with transition metals,[14] have shown that derived potentials are not inordinately sensitive to the atomic generator state so long as highly positive ($\geqslant+5$) or negative ions are not used; these formal oxidation states are not accessible to stable Ln complexes, which is another reason to avoid them. Since lanthanide chemistry is overwhelmingly the chemistry of the trivalent ($+3$) ion, it makes sense to use this state (ground state configuration $1s^2 2s^2 ... 5s^2 5p^6 4f^n$) for the generation of ECPs and valence basis sets. To derive a potential with angular momentum equal to 2 (i.e., a d-potential) numerical DHF calculations were carried out on the $+2$ ($1s^2 2s^2 ... 5s^2 5p^6 4f^n 5d^1$) ion. To simplify the DHF calculations, state-averaged (angular momentum and spin) wave functions were used.

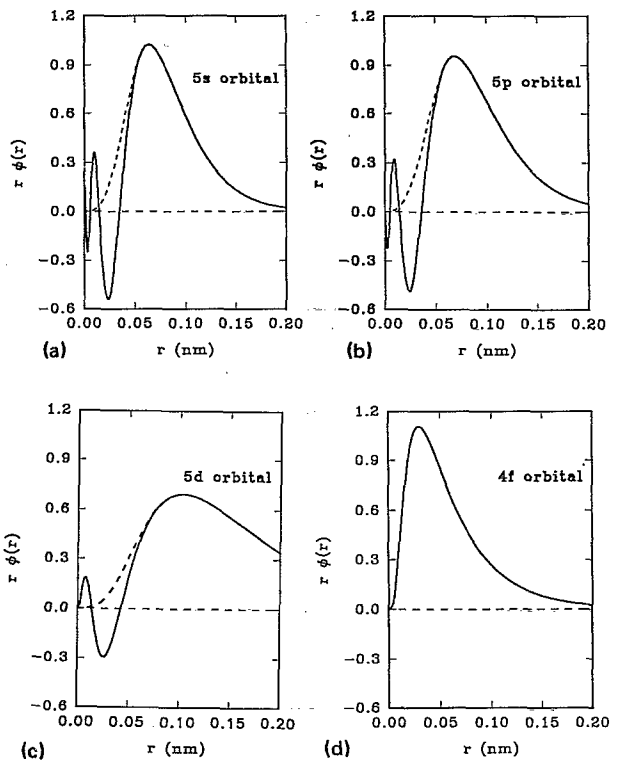

FIG. 1. Plot of the radial function ($r\phi$) vs r (in a.u.) for the (a) 5s; (b) 5p; (c) 5d; and (d) 4f spinor (solid line) and pseudospinor (dashed line) for the multiplet-averaged, Gd^{+3} ($1s^2 2s^2 ... 4f^7$) state.

2. Generation of nodeless pseudospinors

The large components of the numerical, all-electron DHF spinors are converted into nodeless (other than at $r=0$ and ∞) pseudospinors, by means of the shape-consistent procedure of Christiansen *et al.*[16] The normalized, nodeless pseudospinor is generated by splicing together a cubic polynomial and the numerical DHF spinor such that all (n-l-1) nodes in the radial density function are removed. By using this method, the spinor and pseudospinor have the exact same shape after the splicing point, called the match point, which insures good behavior for the pseudospinor in the valence region.

The choice of match point, i.e., the point at which the cubic polynomial is spliced to the DHF spinor is crucial. As with transition metals,[14] the match point was chosen so that it coincides with the outermost maximum in the radial density of the DHF spinor. The overall pseudospinor thus contains no radial nodes (other than at $r=0$ and ∞) and two inflection points, as shown in Figs. 1(a)–1(c) for the typical examples of Gd^{+3} 5s, 5p, and 5d atomic orbitals (AOs). Spinors such as the 4f* (i.e., $4f_{5/2}$) and 4f (i.e., $4f_{7/2}$) which possess only radial nodes at $r=0$ and ∞ are not included in this step [Fig. 1(d)]. Some additional tests were carried out by moving the match point off the outermost radial density maximum, towards and away from the nucleus. Insignificant effects on the derived potentials were found as long as the pseudospinor had the required shape, i.e., no nodes and two inflection points.

3. Generation of relativistic effective potentials and averaged relativistic effective potentials

Following the method of Lee *et al.*,[17] the pseudospinor and eigenvalue are used to generate a numerical potential, by inversion of the Hartree–Fock equations. The numerical potentials, which are j-dependent, are referred to as relativistic effective potentials (REPs). It is possible to use the REPs in quantum calculations. However, for general use the REPs for each particular angular momentum (l) are typically converted to average relativistic effective potentials (AREPs) to remove the j-dependence using the method of Lee *et al.*[18] [Eq. (1)]. Furthermore,

$$V_l^{\mathrm{AREP}} = [\,l V_{l,l-1/2}^{\mathrm{REP}}(r) + (l+1) V_{l,l+1/2}^{\mathrm{REP}}(r)\,] \div (2l+1) \quad (1)$$

it is possible to define an effective spin–orbit coupling operator from the difference in the $j=l+1/2$ and $l=l-1/2$ REPs.[19]

This step in the derivation involves two of the more important choices in an ECP/valence basis set scheme-core size and maximum angular momentum to be used for the ECPs.

The choice of orbitals to include in the core is fraught with uncertainty, particularly in the d- and f-block metals. One needs to strike a balance between chemical accuracy and the desire to replace as many core electrons as possible. From the standpoint of normal chemical reactivity, the 5s and 5p shells can be considered core electrons. Arguments to this effect have also been made for the 4f orbitals.[20]

Dolg *et al.*[12] have looked at various core sizes for some of the lanthanides, while Ross *et al.*[13] have derived potentials with a 54-electron core. For the present case we have chosen a 46-electron core, treating "outer core" 5*s* and 5*p* explicitly for two reasons. First and foremost, we wish to maintain consistency with previous efforts for the transition metals[14] whose chemistry is most closely related to the lanthanides, i.e., the group IIIB metals. For transition metals, inclusion of the *ns* and *np* was essential to reproduce accurate splittings of ground state atomic and ionic states. Dolg *et al.*[12] reach a similar conclusion for the lanthanides. Given the success of this scheme for the transition metals,[11,14] it was decided to treat the 5*s* and 5*p* explicitly. Second, the highly contracted 4*f* AOs have considerable orbital density in the region where the 5*s* and 5*p* have their outermost radial nodes. Since these nodes are removed in the shape-consistent procedure, inaccuracies especially in core-valence exchange integrals might be expected to be significant if the 5*s* and 5*p* are absorbed into the core.

The maximum angular momentum to be used in the AREP arises from the form in which the AREP is cast [Eq. (2)]. The potentials are of two varieties, attractive and repulsive. If the

$$V^{\mathrm{AREP}} = V^{\mathrm{AREP}}_{\mathrm{LMAX}} + \sum_{l=0}^{\mathrm{LMAX}-1} \sum_{m=-l}^{l} (V_l^{\mathrm{AREP}} - V^{\mathrm{AREP}}_{\mathrm{LMAX}}) \times |lm\rangle\langle lm| \qquad (2)$$

angular momentum of the potential is greater than maximum orbital angular momentum occurring in the core (LMAX−1 or $l=2$ for the lanthanides) then the AREP is attractive. In all other cases the potential is repulsive. Furthermore, attractive AREPs (LMAX=3 and higher), which represents core penetration effects without orthogonality, have similar shapes so that a finite sum can be used in Eq. (2). Several comparisons were done in which *f*- and *g*-potentials (the latter derived from spin-averaged $\ldots 5s^2 5p^6 4f^n 5g^1$, Ln^{+2}) were compared for various lanthanides. The *f*- and *g*-potentials are similar enough in shape to obviate the additional computational expense of employing *g*-potentials. Note also from Eq. (2) that we have represented the AREPs with angular momentum lower than LMAX in the standard difference notation, $V_{\mathrm{l-LMAX}}$.

4. Generation of analytical representation for the pseudoorbitals

At this point, it is possible to take the numerical potential and obtain an analytical function for use in molecular calculations by fitting with an expansion of functions, such as Gaussians.[21] Following the lead of the transition metals[14] we have chosen to circumvent the least-squares step and follow a procedure which allows us to avoid using a large number of Gaussians (>6) to fit the numerical potential.

We use the numerical ECPs (AREPs) and a large, even-tempered Gaussian basis set, to generate an analytical form of the pseudo-orbital (exponents are fixed but coefficients are optimized within the constraints of the variational principle).[22] At this point we should note that the same generator states (Ln^{+3}, $4f^n$ to generate the *s*, *p*, and *f* potentials and Ln^{+2}, $4f^n 5d^1$ to generate the *d* potential) are used here as in the DHF step. The only difference is that the *j*-dependency arising from spin–orbit coupling has been "averaged" away using Eq. (1) so that DHF pseudospinors are replaced with pseudo-orbitals. The large (12 function), even-tempered (multiplicative factor of 2) basis set was expanded about the exponent for the best, one-Gaussian fit to the pseudo-orbital. Eigenvalues and eigenvector obtained thusly, the latter in analytical form, are "exact" values, which will subsequently be reproduced with more compact, analytical ECPs and basis sets.

5. Generation of analytical forms for the potentials

Using the "exact" analytical eigenfunctions and eigenvalues, analytical form of the potentials are generated by the method originally proposed by Barthelat *et al.*[23] and later employed successfully by Stevens *et al.*[14] As elsewhere there is a need to balance computational effort with desired accuracy. The more compact the potentials can be made, the greater the savings in computational effort when the derived potentials are used in *ab initio* calculations. On the other hand, agreement between the "exact" and optimized values should be as close as possible. The optimization process was achieved by minimization of the functional $\|O\|$ in Eq. (3), where quantities capped by a tilde are those being optimized while the others are the

$$\|O\| = [\langle X_l | O^2 | X_l \rangle]^{1/2}, \qquad (3a)$$

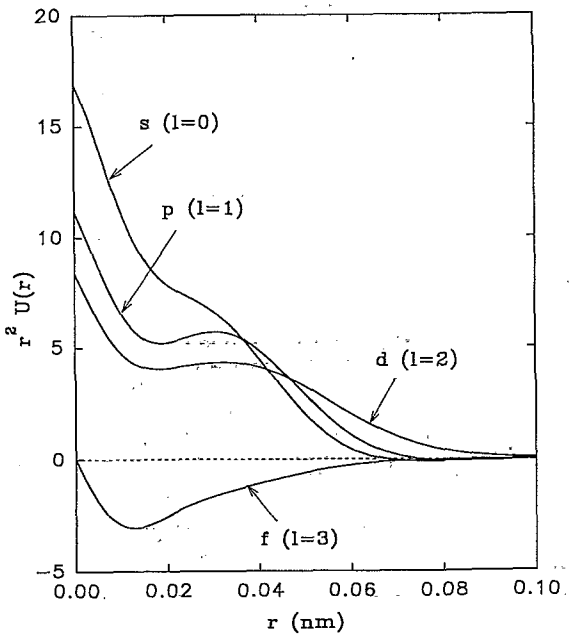

FIG. 2. Plot of $r^2U(r)$ for the various angular momentum potentials of the multiplet-averaged, Gd^{+3} ($1s^2 2s^2 \ldots 4f^7$) state.

$$O=\tilde{\epsilon}_l|\tilde{X}_l\rangle\langle\tilde{X}_l|-\epsilon_l|X_l\rangle\langle X_l| \quad (3b)$$

"exact" solutions from the previous step. In keeping with the criterion settled upon previously,[14] the optimization process was continued until the overlap between the "exact" and trial pseudo-orbital was 0.999 99 or greater, and the difference in the "exact" and trial eigenvalues was ~0.001 a.u. The potentials have the form given in Eq. (4),

$$r^2V_l(r)=\sum_k A_{l,k}r^{n_{l,k}}e^{-B_{l,k}r^2}. \quad (4)$$

The V_f potentials were optimized first, and then other angular momentum potentials were optimized with the analytic V_f potential subtracted. The potentials thus produced have the general shapes shown in Fig. 2. The parameters defining the potentials are collected in Table I. To achieve consistency within the series, previous results for lanthanum ($Z=57$) (Ref. 14) were used as an initial guess for Ce ($Z=58$); each succeeding lanthanide used the optimized ECPs from the previous lanthanide as a starting guess.

6. Generation of optimized valence basis sets

One can assemble the following orbitals for inclusion in the lanthanide valence basis set, 5*s*, 5*p*, 4*f*, 5*d*, 6*s*, and 6*p*. The first two AOs are completely occupied in all chemically reasonable oxidation states for the lanthanides. The final three AOs will be unoccupied in the prevalent +3 ion. The ground state for the +3 ion is f^n with n ranging from 1 (for Ce^{+3}) to 14 (Lu^{+3}). Since it is the most important state, the +3 ($5s^25p^64f^n$) ion was used to optimize basis sets for the 5*s*, 5*p*, and 4*f* AOS. The Ln^{+2} ($5s^25p^64f^n5d^1$) state was used to optimize the *d* basis set. The Ln^{+2} ($5s^25p^64f^n6s^1$) state was used to optimize a 6*s* basis augmentating the previously optimized 5*s* basis.

Since the lowest energy $4f^n$ configuration is invariably high-spin, this multiplet was used for energy optimization of the basis sets. Derivation of the ECPs used multiplet-averaged configurations since the derived potentials are not sensitive to the exact spin-state so much as the oxidation state, and the use of the multiplet-averaged configuration allows certain advantages in speed and facility. The valence basis sets will be more sensitive to the spin-coupling scheme, since higher-energy spin-states can have diffuse and Rydberg character, necessitating larger Gaussian expansions. The high-spin Ln^{+2} ($5s^25p^64f^n5d^1$) and Ln^{+2} ($5s^25p^64f^n6s^1$) states were also used where appropriate.

For the *s* manifold a quadruple zeta representation (Table II) of Gaussian-type orbitals (GTOs) was found to be necessary to obtain optimized energies within 0.001–0.003 a.u. of large, even-tempered basis set results. These four Gaussian sets are represented as 3,1 contractions in Table II. In all cases, *ns* and *np* shells were assumed to have the same exponents due to their similar radial extent for the same principal quantum number. For the *d* manifold, a three GTO fit yields eigenfunctions which are <0.001 a.u. different from large, even-tempered results. We have listed these in Table II as a normalized set of three optimized GTOs.

The 4*f* orbitals proved to be the most difficult of all to obtain compact basis set representation, due to their peculiar nature, which in turn is responsible for many of the interesting spectroscopic and magnetic properties of the lanthanides. The 4*f* orbitals do not decay as rapidly at large distances from the nucleus, as do most orbitals, e.g., the 5*s* and 5*p*, which have maxima so close to the nucleus. The result is that although the predominant portion of electron density is at $r<0.5$ Å (Fig. 3) the 4*f* still have appreciable tails in the range of $r>2$ Å! These long range "tails" are not significant in ordinary chemical reactivity (at least as pertains to the degree of covalency in typical Ln-ligand bonds), but are probably important in terms of the spectroscopic and magnetic properties of the lanthanides. Since the lanthanide 4*f* changes across the series (Fig. 3) the number of Gaussians needed to achieve energies close (1–10 mhartrees) to the large, even-tempered results also change. For the early, middle, and late lanthanide series, the number of Gaussians needed were 6, 7, and 8, respectively. To achieve consistency throughout it was decided to use the compromise value of 7 GTOs for the entire series. The optimized 7 GTO fits for the 4*f* orbitals are listed in Table II.

B. Application of the derived ECPs and valence basis sets to atomic problems

The various portions of the derivation process as we have seen constitute a trade-off between accuracy and compactness. In this regard, two approximations are of concern. First, the replacement of the numerical potential with an analytical representation. Second, the replacement of the large, even-tempered basis sets with shorter, more compact optimized basis sets. As stated above, the basis sets and ECPs were optimized for the appropriate high-spin +3 and +2 oxidation states, thus tests on these states can be considered a best case scenario for testing the accuracy of these two approximations. Despite the fact that the chemistry of the lanthanides is dominated by a small selection of spin and oxidation states, it is still necessary to assess the flexibility of the derived potentials and basis sets. To this end, we have compared multiplet-averaged calculations at various levels as well as looked at the relative energetics of the +2 and +3 states. Given the fact that the basis sets were not optimized for these states, this latter series of tests can be considered as a worse case scenario.

In Table III, we have compared the calculated eigenvalues for four sets of calculations, analytical potential/optimized basis set; numerical potential/large, even-tempered basis; analytical potential/large, even-tempered basis; numerical Dirac–Fock calculations. For the sake of brevity, representative results are shown for early (Ce^{+2}), middle (Gd^{+2}), and late (Lu^{+2}) lanthanide ions. All results in Table III are for the multiplet-averaged

TABLE I. Lanthanide effective core potentials.[a]

	A_{lk}	n_{lk}	B_{lk}		A_{lk}	n_{lk}	B_{lk}
Ce-ECP				Pm-ECP			
$V(f)$				$V(f)$			
	−15.348 756 1	1	9.207 479 30		−15.586 755 7	1	11.106 708 4
	−5.843 239 53	1	1.867 301 16		−6.012 034 57	1	2.210 447 87
$V(s\text{-}f)$				$V(s\text{-}f)$			
	−255.562 383	2	1.893 701 34		−215.581 787	2	2.273 653 12
	307.313 928	2	1.979 148 59		277.534 042	2	2.405 029 52
	10.669 901 7	0	10.742 969 7		11.559 801 2	0	10.764 731 0
$V(p\text{-}f)$				$V(p\text{-}f)$			
	12.229 210 9	0	7.755 929 79		10.336 664 6	0	9.853 977 00
	124.942 466	2	1.815 641 26		121.467 693	2	2.076 268 90
	−84.599 986 8	2	1.671 647 19		−74.876 644 0	2	1.864 934 86
$V(d\text{-}f)$				$V(d\text{-}f)$			
	24.944 675 5	2	1.706 420 47		28.486 110 4	2	1.977 982 21
	10.286 144 7	0	6.489 337 42		9.280 905 76	0	6.673 294 17
Pr-ECP				Sm-ECP			
$V(f)$				$V(f)$			
	−15.443 521 9	1	9.829 728 56		−15.658 620 1	1	11.758 123 9
	−5.896 112 85	1	1.980 700 77		−6.053 764 96	1	2.328 082 97
$V(s\text{-}f)$				$V(s\text{-}f)$			
	−223.643 982	2	2.129 555 79		−206.067 266	2	2.377 766 11
	278.134 515	2	2.227 465 46		270.342 598	2	2.524 715 90
	12.621 071 8	0	7.283 719 63		11.444 904 4	0	10.264 389 8
$V(p\text{-}f)$				$V(p\text{-}f)$			
	12.525 639 0	0	7.809 280 39		10.695 100 7	0	10.005 423 6
	121.952 782	2	1.929 778 61		121.877 228	2	2.201 241 25
	−79.404 751 2	2	1.764 789 25		−72.788 390 3	2	1.968 092 83
$V(d\text{-}f)$				$V(d\text{-}f)$			
	26.192 665 2	2	1.797 974 32		29.523 940 0	2	2.067 204 39
	9.873 912 06	0	6.548 051 53		9.037 177 01	0	6.712 889 04
Nd-ECP				Eu-ECP			
$V(f)$				$V(f)$			
	−15.483 004 4	1	10.429 788 4		−15.724 479 9	1	12.418 353 9
	−5.948 333 67	1	2.092 291 28		−6.091 073 68	1	2.447 558 47
$V(s\text{-}f)$				$V(s\text{-}f)$			
	−219.470 840	2	2.224 785 61		−196.637 738	2	2.503 828 45
	280.528 928	2	2.344 595 86		264.103 449	2	2.669 264 10
	11.762 325 0	0	11.857 983 0		11.806 980 2	0	10.367 382 4
$V(p\text{-}f)$				$V(p\text{-}f)$			
	11.436 121 7	0	9.443 064 51		10.938 060 1	0	10.134 183 1
	120.335 356	2	1.989 490 76		128.160 269	2	2.324 399 41
	−75.781 964 3	2	1.798 054 46		−76.515 327 6	2	2.083 374 87
$V(d\text{-}f)$				$V(d\text{-}f)$			
	27.383 071 3	2	1.888 550 52		30.467 326 4	2	2.154 389 42
	9.617 410 49	0	6.643 665 54		8.741 226 93	0	6.693 797 32
Gd-ECPs				Ho-ECPs			
$V(f)$				$V(f)$			
	−15.786 726 0	1	13.095 090 8		−15.951 658 8	1	15.214 140 8
	−6.127 778 14	1	2.569 738 56		−6.231 625 68	1	2.951 249 16
$V(s\text{-}f)$				$V(s\text{-}f)$			
	−137.902 125	2	2.702 265 23		−110.583 011	2	2.847 456 82
	208.964 540	2	2.933 477 41		192.701 733	2	3.224 215 98
	16.858 693 6	0	9.850 809 64		11.354 686 5	0	16.156 188 1
$V(p\text{-}f)$				$V(p\text{-}f)$			
	11.130 834 3	0	10.256 201 2		10.842 743 3	0	9.926 083 26
	131.651 321	2	2.452 732 13		116.520 060	2	2.862 307 17
	−77.444 300 8	2	2.196 934 27		−55.661 098 0	2	2.472 449 17
$V(d\text{-}f)$				$V(d\text{-}f)$			
	31.466 411 8	2	2.247 169 23		33.342 490 6	2	2.491 155 11
	8.345 072 86	0	6.430 643 69		7.730 049 15	0	6.351 009 11
Tb-ECPs				Er-ECPs			
$V(f)$				$V(f)$			
	−15.840 808 1	1	13.784 988 0		−16.004 358 2	1	15.959 653 1
	−6.166 784 75	1	2.693 866 93		−6.265 094 74	1	3.085 058 24

TABLE I. (*Continued.*)

	A_{lk}	n_{lk}	B_{lk}		A_{lk}	n_{lk}	B_{lk}
$V(s\text{-}f)$				$V(s\text{-}f)$			
	−140.103 224	2	2.618 173 46		−150.367 002	2	3.036 185 26
	215.289 935	2	2.890 417 97		236.197 756	2	3.352 534 76
	11.681 233 7	0	17.048 971 3		11.416 461 1	0	16.039 240 0
$V(p\text{-}f)$				$V(p\text{-}f)$			
	11.121 621 3	0	10.125 331 4		11.892 535 8	0	11.046 346 3
	139.657 131	2	2.565 703 77		130.543 501	2	3.017 991 14
	−83.309 822 1	2	2.308 348 41		−65.692 298 8	2	2.647 271 81
$V(d\text{-}f)$				$V(d\text{-}f)$			
	32.121 767 9	2	2.326 033 32		33.731 807 6	2	2.570 087 55
	8.223 362 56	0	6.593 118 02		7.488 689 13	0	6.165 640 70
Dy-ECPs				Tm-ECPs			
$V(f)$				$V(f)$			
	−15.897 237 0	1	14.490 581 7		−16.055 361 7	1	16.724 355 4
	−6.199 393 99	1	2.821 051 35		−6.298 329 35	1	3.222 161 96
$V(s\text{-}f)$				$V(s\text{-}f)$			
	−130.004 348	2	2.739 081 05		−143.245 953	2	3.183 383 03
	208.636 024	2	3.049 347 14		233.195 538	2	3.535 314 67
	11.485 466 6	0	16.574 733 0		11.610 944 4	0	16.160 139 2
$V(p\text{-}f)$				$V(p\text{-}f)$			
	11.622 381 3	0	10.694 360 1		7.396 190 33	0	2.463 782 38
	125.415 782	2	2.740 558 34		119.572 429	2	2.721 943 61
	−65.820 382 8	2	2.411 234 63		−84.017 445 3	2	2.495 528 76
$V(d\text{-}f)$				$V(d\text{-}f)$			
	32.797 726 9	2	2.409 613 69		33.841 167 0	2	2.643 616 36
	7.980 231 35	0	6.495 882 52		7.233 500 94	0	5.894 263 45
Yb-ECPS				Lu-ECPs			
$V(f)$				$V(f)$			
	−16.104 975 1	1	17.512 319 0		−16.152 003 8	1	18.320 436 5
	−6.332 779 63	1	3.363 130 57		−6.367 668 16	1	3.507 978 54
$V(s\text{-}f)$				$V(s\text{-}f)$			
	−106.506 399	2	3.299 884 42		−71.317 170 5	2	3.342 248 01
	201.149 552	2	3.771 770 93		169.401 393	2	4.005 094 13
	12.010 016 7	0	16.634 491 7		11.886 115 4	0	16.180 952 1
$V(p\text{-}f)$				$V(p\text{-}f)$			
	7.596 591 44	0	2.655 442 00		7.719 340 58	0	2.721 106 68
	119.649 347	2	2.838 545 81		116.107 363	2	2.982 004 54
	−82.704 696 4	2	2.598 802 32		−78.178 628 4	2	2.714 800 84
$V(d\text{-}f)$				$V(d\text{-}f)$			
	34.171 326 9	2	2.710 264 96		33.911 925 2	2	2.775 711 68
	7.274 862 33	0	6.264 241 86		7.018 710 05	0	5.893 801 26

[a]The analytic form of the effective core potentials is $r^2V(r)=\Sigma A_{lk}\exp(-B_{lk}r^2)r^n_{lk}$.

$5s^25p^64f^n5d^1$ configurations. In general, the trend is that the errors are the least for the early lanthanides [average error in orbital eigenvalues for $Ce^{+2}(5s^25p^64f^15d^1)$ $\approx 0.002\pm0.001$ a.u.] which monotonically increase until at the extreme late lanthanides the average error in eigenvalues is 0.013 ± 0.006 a.u., still quite respectable. In the center, Gd^{+2} [$5s^25p^64f^75d^1$ (spin-averaged) $\approx 0.007\pm0.002$ a.u.] shows excellent agreement. Of interest is the close agreement between the numerical potential/large, even-tempered basis (column 3, Table III) and analytical potential/large, even-tempered basis (column 2, Table III). This demonstrates that most of the deficit is due to basis set. The $4f$ and $5d$ basis sets have been left in their normalized 7 GTO and 3 GTO forms in Table II, so that depending on the accuracy needed for a certain task, they are easily split up, recontracted, and then renormalized or augmented. For molecular calculations, we would suggest splitting the $4f$ and $5d$ to double zeta while leaving the *sp*-shell in its quadruple zeta form. Tests of this contraction scheme for molecular problems are currently being carried out.

A second test compares results for the high-spin +3 cases ($5s^25p^64f^n$) at different levels of theory. Since the basis sets were derived from high-spin states these results are expected to be superior than those summarized for the multiplet averaged state. As before, the agreement is better for the early metals and degrades slightly as one proceeds to the right in the lanthanide series, Table IV. However, results are excellent regardless of position in the lanthanide series. The average error for the entire lanthanide series is only 0.002 ± 0.001 mhartrees. Typical results for $Ce^{+3}(f^1,{}^2F)$, $Gd^{+3}(f^7,{}^8S)$, and $Lu^{+3}(f^{14},{}^1S)$ are listed in Table IV. This excellent agreement is particularly satis-

TABLE II. Optimized lanthanide Gaussian basis sets.[a]

Ce $Z=58$

sp		
3.457 00	3.137 490 6	1.949 716 8
4.291 00	−1.429 516 6	−0.912 311 4
2.290 00	−2.675 848 2	−2.020 037 1
0.285 70	1.000 000 0	1.000 000 0
0.668 40	1.000 000 0	1.000 000 0
0.069 57	1.000 000 0	1.000 000 0
d		
0.591 60	0.278 319 7	
0.300 20	0.458 629 6	
0.124 40	0.396 595 2	
f		
83.880 0	0.005 160 2	
29.970 00	0.043 244 2	
13.050 00	0.140 567 5	
5.727 00	0.271 654 1	
2.549 00	0.385 849 5	
1.075 00	0.356 582 4	
0.398 60	0.191 602 6	

Nd $Z=60$

sp		
5.634 00	−0.706 422 6	−0.581 841 1
4.724 00	1.137 348 0	0.848 716 7
2.064 00	−1.402 933 1	−1.252 379 6
0.772 40	1.000 000 0	1.000 000 0
0.312 70	1.000 000 0	1.000 000 0
0.073 72	1.000 000 0	1.000 000 0
d		
0.677 80	0.279 616 0	
0.325 50	0.479 510 4	
0.132 40	0.381 155 6	
f		
94.380 00	0.005 349 4	
34.330 00	0.042 735 9	
15.210 00	0.138 794 9	
6.816 00	0.267 072 1	
3.096 00	0.380 159 8	
1.330 00	0.357 924 0	
0.492 30	0.194 776 1	

Pr $Z=59$

sp		
3.458 00	0.880 611 4	0.740 362 5
4.921 00	−0.191 756 9	−0.265 742 0
2.100 00	−1.657 958 9	−1.463 678 1
0.729 00	1.000 000 0	1.000 000 0
0.299 40	1.000 000 0	1.000 000 0
0.071 79	1.000 000 0	1.000 000 0
d		
0.641 90	0.274 419 9	
0.315 70	0.473 027 1	
0.129 00	0.389 927 5	
f		
88.460 00	0.005 367 6	
32.000 00	0.043 336 7	
14.090 00	0.140 158 9	
6.246 00	0.270 863 2	
2.808 00	0.383 417 0	
1.198 00	0.355 403 9	
0.445 10	0.191 412 4	

Pm $Z=61$

sp		
8.289 00	−0.064 775 5	−0.078 534 2
3.856 00	0.530 092 0	0.397 554 2
2.123 00	−1.438 678 1	−1.302 651 2
0.820 50	1.000 000 0	1.000 000 0
0.325 50	1.000 000 0	1.000 000 0
0.075 54	1.000 000 0	1.000 000 0
d		
0.718 90	0.260 562 6	
0.344 90	0.481 304 2	
0.137 00	0.401 467 4	
f		
101.100 00	0.005 287 9	
36.860 00	0.041 977 6	
16.430 00	0.136 275 3	
7.445 00	0.261 166 1	
3.414 00	0.375 756 8	
1.472 00	0.362 903 4	
0.539 60	0.202 602 1	

Sm $Z=62$

sp		
12.610 00	−0.014 999 6	−0.031 579 4
3.278 00	0.718 778 8	0.509 098 8
2.238 00	−1.678 150 0	−1.464 062 4
0.866 10	1.000 000 0	1.000 000 0
0.337 40	1.000 000 0	1.000 000 0
0.077 32	1.000 000 0	1.000 000 0
d		
0.785 10	0.257 405 3	
0.362 20	0.459 234 0	
0.157 30	0.419 376 7	
f		
83.760 00	0.009 831 0	
30.540 00	0.069 045 1	
13.160 00	0.189 673 0	
5.730 00	0.331 588 3	
2.585 00	0.373 345 2	
1.134 00	0.286 865 9	
0.444 50	0.132 924 9	

Gd $Z=64$

sp		
17.240 00	0.003 607 0	−0.020 728 7
3.346 00	0.737 570 6	0.519 148 7
2.429 00	−1.714 927 8	−1.488 382 2
0.934 90	1.000 000 0	1.000 000 0
0.358 80	1.000 000 0	1.000 000 0
0.081 05	1.000 000 0	1.000 000 0
d		
0.857 30	0.199 229 9	
0.412 80	0.483 035 7	
0.151 90	0.468 083 3	
f		
77.600 00	0.015 420 3	
28.610 00	0.093 934 1	
12.130 00	0.229 645 8	
5.239 00	0.370 284 7	
2.305 00	0.363 612 4	
0.994 20	0.235 616 5	
0.403 10	0.088 127 9	

TABLE II. (*Continued.*)

Eu $Z=63$

sp		
14.220 00	−0.009 005 5	−0.026 102 1
3.237 00	0.842 326 9	0.578 079 3
2.344 00	−1.808 082 6	−1.540 346 5
0.904 70	1.000 000 0	1.000 000 0
0.348 60	1.000 000 0	1.000 000 0
0.079 16	1.000 000 0	1.000 000 0
d		
0.815 40	0.218 776 1	
0.399 10	0.478 198 3	
0.151 10	0.449 585 0	
f		
83.900 00	0.011 252 2	
30.660 00	0.076 056 4	
13.170 00	0.200 792 4	
5.745 00	0.341 486 9	
2.588 00	0.369 757 4	
1.134 00	0.273 568 6	
0.447 20	0.121 768 6	

Tb $Z=65$

sp		
13.180 00	−0.039 805 8	−0.032 682 1
3.847 00	0.780 611 1	0.397 984 7
2.537 00	−1.715 852 8	−1.356 054 0
0.961 40	1.000 000 0	1.000 000 0
0.369 70	1.000 000 0	1.000 000 0
0.082 54	1.000 000 0	1.000 000 0
d		
0.902 50	0.181 507 0	
0.424 80	0.485 237 6	
0.152 10	0.487 725 1	
f		
90.720 00	0.012 114 3	
33.170 00	0.079 914 6	
14.330 00	0.204 133 1	
6.357 00	0.335 574 3	
2.914 00	0.360 039 7	
1.286 00	0.276 447 5	
0.498 50	0.130 553 1	

Dy $Z=66$

sp		
12.360 00	−0.046 979 0	−0.039 331 1
4.155 00	0.723 122 9	0.366 659 6
2.647 00	−1.650 975 7	−1.319 020 7
0.992 90	1.000 000 0	1.000 000 0
0.380 80	1.000 000 0	1.000 000 0
0.084 08	1.000 000 0	1.000 000 0
d		
0.924 40	0.184 312 6	
0.428 00	0.483 081 0	
0.152 30	0.490 414 5	
f		
97.470 00	0.011 510 8	
35.710 00	0.076 415 8	
15.580 00	0.196 494 3	
7.006 00	0.322 523 0	
3.259 00	0.356 982 7	
1.440 00	0.290 646 9	
0.545 70	0.146 161 3	

Er $Z=68$

sp		
12.580 00	−0.042 558 7	−0.040 282 9
4.449 00	0.717 933 6	0.357 717 9
2.873 00	−1.650 289 4	−1.311 041 3
1.058 00	1.000 000 0	1.000 000 0
0.402 50	1.000 000 0	1.000 000 0
0.087 08	1.000 000 0	1.000 000 0
d		
0.979 10	0.192 369 9	
0.436 70	0.485 746 9	
0.154 40	0.485 494 0	
f		
105.100 00	0.012 127 7	
38.680 00	0.078 436 8	
17.000 00	0.197 229 9	
7.745 00	0.317 212 3	
3.642 00	0.351 524 1	
1.608 00	0.294 457 0	
0.598 00	0.153 976 1	

Ho $Z=67$

sp		
12.310 00	−0.045 497 9	−0.038 314 6
4.305 00	0.710 566 1	0.347 927 2
2.749 00	−1.640 100 6	−1.302 166 1
1.024 00	1.000 000 0	1.000 000 0
0.391 40	1.000 000 0	1.000 000 0
0.085 55	1.000 000 0	1.000 000 0
d		
0.950 70	0.188 633 7	
0.431 70	0.484 323 6	
0.153 10	0.487 894 1	
f		
104.900 00	0.010 848 2	
38.500 00	0.072 703 4	
16.950 00	0.188 682 1	
7.725 00	0.309 931 6	
3.635 00	0.355 762 0	
1.602 00	0.303 952 7	
0.594 80	0.159 998 7	

Tm $Z=69$

sp		
11.040 00	−0.059 272 9	−0.024 281 8
4.881 00	0.611 570 2	0.216 124 1
2.928 00	−1.527 704 5	−1.182 557 6
1.080 00	1.000 000 0	1.000 000 0
0.412 10	1.000 000 0	1.000 000 0
0.088 51	1.000 000 0	1.000 000 0
d		
1.009 00	0.193 803 9	
0.442 70	0.486 833 4	
0.155 60	0.485 761 6	
f		
113.400 00	0.011 283 6	
41.800 00	0.073 983 3	
18.530 00	0.188 635 8	
8.547 00	0.304 786 9	
4.056 00	0.352 225 7	
1.779 00	0.308 121 7	
0.647 80	0.167 033 0	

TABLE II. (*Continued.*)

Yb $Z=70$			Lu $Z=71$		
sp			*sp*		
10.080 00	−0.089 068 1	−0.035 928 1	9.469 00	−0.111 900 4	−0.046 391 5
5.395 00	0.576 740 9	0.194 135 7	5.568 00	0.632 141 4	0.217 913 0
3.031 00	−1.462 892 4	−1.149 982 5	3.182 00	−1.495 171 2	−1.163 416 1
1.108 00	1.000 000 0	1.000 000 0	1.135 00	1.000 000 0	1.000 000 0
0.422 10	1.000 000 0	1.000 000 0	0.432 00	1.000 000 0	1.000 000 0
0.090 08	1.000 000 0	1.000 000 0	0.091 61	1.000 000 0	1.000 000 0
d			*d*		
1.051 00	0.187 718 0		1.101 00	0.169 956 2	
0.451 90	0.487 369 5		0.463 90	0.484 498 7	
0.156 20	0.495 038 9		0.156 40	0.518 336 5	
f			*f*		
122.500 00	0.010 448 8		117.800 00	0.012 819 5	
45.180 00	0.069 537 4		43.400 00	0.081 385 7	
20.200 00	0.179 891 6		19.130 00	0.200 669 2	
9.428 00	0.293 145 0		8.797 00	0.315 672 8	
4.501 00	0.353 651 3		4.153 00	0.348 534 9	
1.960 00	0.320 695 5		1.817 00	0.294 638 5	
0.700 50	0.179 317 0		0.661 70	0.157 145 2	

[a]Optimized Gaussian exponents (column 1) and normalized contraction coefficients (column 2) for lanthanide valence basis sets. For the *sp* shell, the same exponents were used, but with different contraction coefficients. The normalized contraction coefficients for *s* shell are given in column 2 and those for the *p* shell are given in column 3.

fying since the high-spin $+3$ (f^n) state is overwhelmingly the state of interest in lanthanide chemistry.

As a final test of the derived potentials the multiplet-average results for $+3$ (f^n) and $+2$ ($f^n d^1$) were used to calculate the energy change for the ionization process in Eq. (5). By

$$\mathrm{Ln}^{+2}(4f^n5d^1) \rightarrow \mathrm{Ln}^{+3}(4f^n) + e^- \qquad (5)$$

using the multiplet-averaged states we have the chance to compare energies with those derived from accurate DHF results. These results are collected in Table V for the entire series. Once again, excellent agreement is found using the compact ECPs and their optimized basis sets. Errors in the

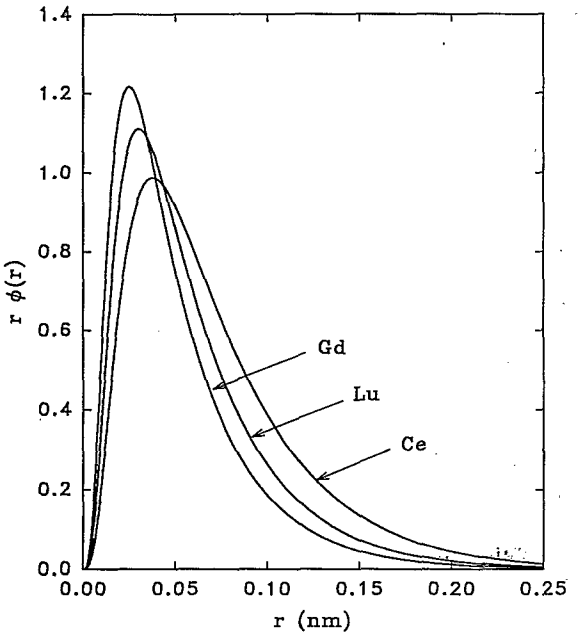

FIG. 3. Plot of the radial function ($r\phi$) vs r (in a.u.) showing the changes in the $4f$ orbital upon proceeding from an early (Ce^{+3}) to middle (Gd^{+3}) to late (Lu^{+3}) lanthanide ion.

TABLE III. Comparison of results for spin-averaged $\mathrm{Ln}^{+2}(5s^25p^64f^n5d^1)$.[a]

	$V_{\text{analytical}}$/ optzd. basis ϵ_i	$V_{\text{analytical}}$/ large basis ϵ_i	$V_{\text{numerical}}$/ large basis ϵ_i	DHF ϵ_i
Ce(5*s*)[b]	−2.3376	−2.3403	−2.3364	−2.3369
Ce(5*p*)	−1.5410	−1.5429	−1.5413	−1.5418
Ce(5*d*)	−0.6785	−0.6806	−0.6803	−0.6809
Ce(4*f*)[c]	−1.0012	−1.0025	−1.0024	−0.9947
Gd(5*s*)	−2.7314	−2.7402	−2.7382	−2.7398
Gd(5*p*)	−1.7395	−1.7463	−1.7440	−1.7493
Gd(5*d*)	−0.6982	−0.7031	−0.7020	−0.7042
Gd(4*f*)[d]	−1.2126	−1.2223	−1.2229	−1.2173
Lu(5*s*)	−3.2086	−3.2225	−3.2184	−3.2251
Lu(5*p*)	−1.9534	−1.9642	−1.9604	−1.9743
Lu(5*d*)	−0.6992	−0.7052	−0.7025	−0.7080
Lu(4*f*)[e]	−1.3268	−1.3456	−1.3457	−1.3478

[a]This table presents a comparison of pseudo-orbital eigenvalues determined with different basis sets (large, even-tempered and the smaller, optimized valence basis) and potentials (numerical and analytical). The DHF eigenvalues in column 4 are the weighted-average of the *j*-dependent spinors.

[b]The orbital eigenvalues (ϵ_i) are reported in atomic units.

[c]The average deviation between the analytical ECP, optimized basis set results, and those at other levels of approximation for Ce^{+2} ($5s^25p^64f^15d^1$, spin-averaged) is $0.002+0.001$ a.u.

[d]The average deviation between the analytical ECP, optimized basis set results, and those at other levels of approximation for Gd^{+2} ($5s^25p^64f^75d^1$, spin-averaged) is $0.007+0.002$ a.u.

[e]The average deviation between the analytical ECP, optimized basis set results, and those at other levels of approximation for Lu^{+2} ($5s^25p^64f^{14}5d^1$, spin-averaged) is $0.013+0.006$ a.u.

TABLE IV. Comparison of results for high-spin $Ln^{+3}(5s^25p^64f^n)$.[a]

	$V_{analytical}$/ optzd. basis ϵ_i	$V_{analytical}$/ large basis ϵ_i	$V_{numerical}$/ large basis ϵ_i
Ce(5s)[b]	−2.7154	−2.7142	−2.7115
Ce(5p)	−1.9029	−1.8971	−1.9008
Ce(4f)[c]	−1.3855	−1.3826	−1.3849
Gd(5s)	−3.1354	−3.1349	−3.1329
Gd(5p)	−2.1294	−2.1284	−2.1263
Gd(4f)[d]	−1.7429	−1.7420	−1.7423
Lu(5s)	−3.6546	−3.6586	−3.6551
Lu(5p)	−2.3809	−2.3835	−2.3803
Lu(4f)[e]	−1.7753	−1.7803	−1.7810

[a]This table presents a comparison of pseudo-orbital eigenvalues determined with different basis sets (large, even-tempered and the smaller, optimized valence basis) and potentials (numerical and analytical).
[b]The orbital eigenvalues (ϵ_i) are reported in atomic units.
[c]The average deviation between the analytical ECP, optimized basis set results, and those at other levels of approximation for Ce^{+3} ($5s^25p^64f^1$, high-spin) is 0.003+0.002 a.u.
[d]The average deviation between the analytical ECP, optimized basis set results, and those at other levels of approximation for Gd^{+3} ($5s^25p^64f^7$, high-spin) is 0.002+0.001 a.u.
[e]The average deviation between the analytical ECP, optimized basis set results, and those at other levels of approximation for Lu^{+3} ($5s^25p^64f^7$, high-spin) is 0.003+0.002 a.u.

ionization energies range from 0.002 a.u. for Ce and Pr to 0.007 a.u. for Lu. Thus, the derived scheme shows good energetic results not only for a single state of the lanthanides, but good energetic separation between two states.

III. CONCLUSIONS AND SUMMARY

We have presented in this contribution a collection of compact effective core potentials and matching valence basis sets for the lanthanides (Ce to Lu). The goal was to derive a consistent set of ECPs for the entire series, consistent not only within the lanthanide series, but also with the third-row transition metals which are their chemical cousins. The choices made in the derivation process were discussed. In the main, these choices were based on the known chemistry of the lanthanides (e.g., the predominance of the +3 ion) and the successful precedents of the transition metals.[14] Additional tests of the finer points (e.g., the order of the polynomial used in the shape-consistent procedure) were also carried out. The 5s and 5p are treated as "outer" core and all lower energy AOs are replaced with the ECP, giving rise to a 46-electron core. Generator states were chosen to be the most chemically relevant +3 and +2 states. Two approximations are made in the derivation of the ECP to get them into useful form. First, the numerical potential is replaced with an analytic function, which is as compact as possible. Second, large, even-tempered basis sets are replaced with smaller optimized basis sets. Results for the atoms indicate that the greatest error vs numerical potential/large, even-tempered basis set calculations result from the basis sets. Thus, one could easily change the contraction pattern or augment with extra functions depending on whether one wanted a qualitative understanding of a reaction potential energy surface or highly accurate calculation of spectroscopic properties. In any case, deviations are small and they do realize a great savings in the time of the calculation. The good agreement found in atomic calculations is encouraging since the highly ionic nature of the bonding in lanthanides[20] means that the central Ln^{+3} species is essentially an atomic ion being slightly perturbed by the ligand field. It is expected that the compact representation of the ECPs and valence basis sets will eventually encourage their use in molecular calculations. Presently, we are working to extend the testing of this scheme to molecular complexes of the lanthanides.

TABLE V. Calculated transition energies.[a]

	ΔE(DHF)[b]	ΔE(ECP)[c]	δ[d]
Ce	0.6726	0.6712	2
Pr	0.6785	0.6757	2
Nd	0.6836	0.6797	4
Pm	0.6872	0.6828	4
Sm	0.6908	0.6854	6
Eu	0.6934	0.6888	4
Gd	0.6955	0.6910	4
Tb	0.6972	0.6923	5
Dy	0.6980	0.6933	5
Ho	0.6988	0.6937	5
Er	0.6997	0.6941	5
Tm	0.6995	0.6939	5
Yb	0.6994	0.6929	6
Lu	0.6999	0.6928	7

[a]The calculated energies are for the process Ln^{+2} ($5s^25p^64f^n5d^1$, spin-averaged) → Ln^{+3} ($5s^25p^64f^n$, spin-averaged) + e^-.
[b]The values ΔE(DHF), in atomic units, were calculated with the numerical, Dirac–Hartree–Fock program due to Desclaux (Ref. 15).
[c]The values ΔE(ECP), in atomic units, were calculated using the derived analytical ECPs and optimized basis sets.
[d]The difference, to the nearest thousandth of an atomic unit, between the DHF and ECP results.

ACKNOWLEDGMENTS

The work described herein was carried out while one of the authors (T.R.C.) was a Visiting Scientist at the Center for Advanced Research in Biotechnology (CARB). T.R.C. would like to thank the CARB family for their hospitality during his stay. This research was funded by a grant from the National Institutes of Standards and Technology (in the form of an Intergovernmental Personnel Assignment) and a Faculty Research Grant (from Memphis State University) to T.R.C. The derivation of the ECPs was greatly assisted by the performance of several of the larger test calculations at the San Diego Supercomputer Center, administered by the National Science Foundation. The assistance of Harold Basch (Department of Chemistry, Bar-Ilan University) and Morris Krauss (NIST) with the various computer programs is gratefully acknowledged, as are useful and informative discussions with Rick Ross (PPG Industries, Inc.).

[1] G. Jeske, H. Lauke, H. Mauermann, H. Schumann, and T. J. Marks, J. Am. Chem. Soc. **107**, 8111 (1985).
[2] P. L. Watson and G. W. Parshall, Acc. Chem. Res. **18**, 51 (1985).
[3] C. N. R. Rao and B. Raveau, Acc. Chem. Res. **22**, 106 (1989).
[4] W. DeW. Horrocks, Jr. and M. Albin, Prog. Inorg. Chem. **31**, 1 (1984).
[5] R. B. Lauffer, Chem. Rev. **87**, 901 (1987).
[6] M. C. Zerner and D. Salahub, *The Challenge of d- and f-Electrons* (American Chemical Society, Washington, D.C., 1989).
[7] A. Veillard, *Quantum Chemistry: The Challenge of Transition Metals and Coordination Chemistry* (Reidel, Dordrecht, 1989).
[8] R. Hoffmann and J. V. Ortiz, Inorg. Chem. **24**, 2095 (1985); R. Hoffmann, J. Y. Saillard, and H. Rabaâ, J. Am. Chem. Soc. **108**, 4327 (1986).
[9] J. C. Culberson, P. Knappe, N. Rosch, and M. C. Zerner, Theor. Chim. Acta **71**, 21 (1987); R. Jing-Qing and X. Gaung-Xian, Int. J. Quantum Chem. **29**, 1017 (1986).
[10] P. Pyykko and J. P. Desclaux, Chem. Phys. **34**, 261 (1978).
[11] A typical application of the ECP scheme of Stevens *et al.* (Ref. 14) to complexes incorporating metals in a variety of coordination numbers and oxidations states can be found in T. R. Cundari, J. Am. Chem. Soc. **114**, 7879 (1992), and references therein.
[12] M. Dolg and H. Stoll, Theor. Chim. Acta **75**, 369 (1989); M. Dolg, H. Stoll, and H. Preuss, J. Chem. Phys. **90**, 1730 (1989).
[13] R. B. Ross, S. Gayen, and W. C. Ermler (to be submitted).
[14] W. J. Stevens, M. Krauss, H. Basch, and P. G. Jasien, Can. J. Chem. **70**, 612 (1992).
[15] J. P. Desclaux, Comput. Phys. Commun. **9**, 31 (1975).
[16] P. Christiansen, Y. S. Lee, and K. S. Pitzer, J. Chem. Phys. **71**, 4445 (1979).
[17] Y. S. Lee, W. C. Ermler, and K. S. Pitzer, J. Chem. Phys. **67**, 5861 (1977).
[18] Y. S. Lee, W. C. Ermler, K. S. Pitzer, and A. D. McLean, J. Chem. Phys. **70**, 288 (1979).
[19] This approach was first proposed in W. C. Ermler, Y. S. Lee, P. A. Christiansen, and K. S. Pitzer, Chem. Phys. Lett. **81**, 70 (1981) and applied in W. J. Stevens and M. Krauss, *ibid.* **86**, 320 (1982).
[20] T. J. Marks and R. D. Ernst, in *Comprehensive Organometallic Chemistry*, edited by G. Wilkinson, E. W. Abel, and F. G. A. Stone (Pergamon, Oxford, 1982), Vol. 3, p. 173.
[21] This approach has been used by, among others, P. J. Hay and W. R. Wadt, J. Chem. Phys. **82**, 270, 284, 299 (1985).
[22] The program HFATM performs open- and closed-shell SCF calculations and was written by C. J. Hornback (1967) and modified by H. Basch (1968). The ability to handle numerical potentials was programmed in 1983 by W. J. Stevens.
[23] J. C. Barthelat, P. Durand, and A. Serafini, Mol. Phys. **33**, 159 (1977).